Article

# Molecular Level Structural Characterization of Self-Assembled Monolayers of Functionalized Bidentate Aromatic Thiols

*Published as part of The Journal of Physical Chemistry virtual special issue "125 Years of The Journal of Physical Chemistry".*

Umit Celik, Han Ju Lee, Terell Keel, Logan A. Swartz, Marshall Van Zijll, Cody J. Chalker, T. Randall Lee,* and Gang-yu Liu*

Read Online

ACCESS | Metrics & More | Article Recommendations | Supporting Information

**ABSTRACT:** While molecular-level structural information is readily available for *n*-alkanethiol self-assembled monolayers (SAMs) on noble metal surfaces, the same cannot be claimed for dithiol-based SAMs due to their lack of long-range-order. This work provides molecular-level structural information on dithiol SAMs by investigating 5-(octyloxy)-1,3-phenylenedimethanethiol (OPDT) SAMs on Au(111) surfaces, using combined high-resolution scanning tunneling microscopy (STM), atomic force microscopy (AFM), and nanolithography. The high coverage OPDT SAMs do not exhibit long-range order. Desorption of these OPDT SAMs leads to the formation of ordered domains known as the striped phases, whose unit mesh is revealed as commensurate with the underlying Au(111) lattice. In these domains, OPDT molecules are lying-down, with the benzene ring and the zigzag plane of the alkyl chain parallel to the Au(111) surface. At the boundaries of these ordered structures, standing-up OPDT molecules are frequently present with an intermolecular space of 1 nm (i.e., 1D ordered structures). Using these ordered structures as internal standards in situ, the structure of the high-coverage OPDT SAMs is revealed: a mixture of standing-up and lying-down molecules randomly distributed on Au(111); as such, these SAMs exhibit little long-range order or ordered domains. The two thiols of each OPDT molecule occupy triple hollow sites on Au(111) surfaces. In the standing-up configuration, the benzene ring is perpendicular to the surface. In the lying-down con-figuration, the benzene ring and zigzag plane of the alkyl chain are parallel to the Au(111) surface. This work represents a high-resolution and molecular-level structural characterization of functionalized dithiol SAMs, furthering our understanding of dithiol molecule−surface interactions and the unique properties of these SAMs.
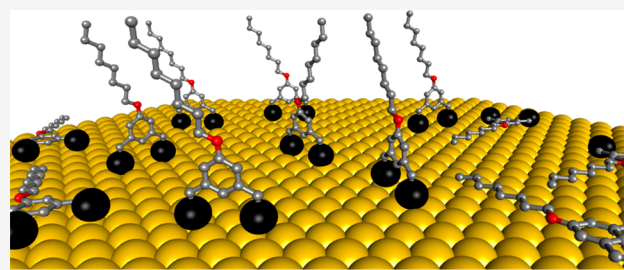
## 1. INTRODUCTION

Self-assembled monolayers (SAMs) generated from dithiol-based adsorbates, such as 5-(octyloxy)-1,3-phenylenedimetha-nethiol (OPDT) shown in Figure 1, have attracted much attention due to their greater thermal stability than their monothiol counterparts.[1,2] The differences in the molecular structure of dithiol versus thiol adsorbates, shown in Figure 1, provide possible rationales for the enhanced stability: namely, the presence of the aromatic ring and the two meta −CH₂−SH groups linked to the ring in the aromatic dithiols. The benzene ring can plausibly give rise to stabilizing π−π interactions among adsorbates in the SAMs, while the two meta thiols provide a chelate effect to the Au(111) surface. The chelating effect, not only stabilizes the SAMs but also inhibits the formation of intramolecular and intermolecular disulfides,[2,3] precursors that lead to the desorption and degradation of SAMs.[4−6] To unveil their enhanced stability and realize advanced applications,[7−9] molecular-level structural characterization of these SAMs becomes essential. While monothiol-based SAMs are well characterized at the molecular level,[10−19] high-resolution investigations of functionalized aromatic dithiol SAMs remain challenging. Prior work indicated that dithiol SAMs on gold surfaces lack long-range order or periodicity,[5,18,20−22] in contrast to *n*-alkanethiol SAMs, which form a closely packed and ordered structure on gold surfaces.[10−16,23] The lack of order makes it technically challenging to achieve molecular-level structural characterization.
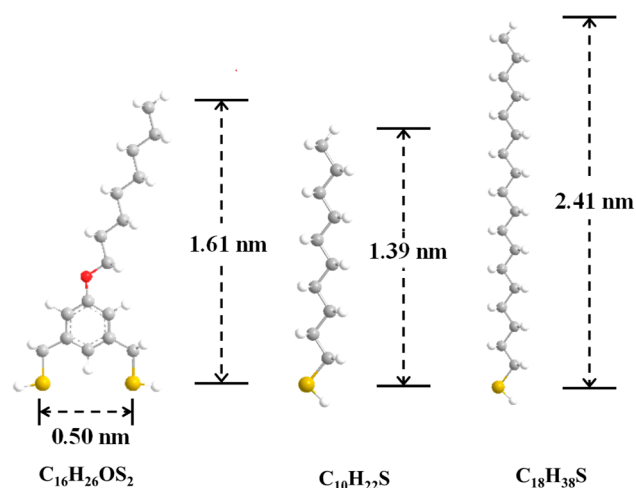
The present study provides a molecular-level structural characterization of OPDT SAMs on Au(111) surfaces using a combination of high-resolution imaging and nanolithography
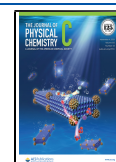
**Figure 1.** Structure of an aromatic dithiol, OPDT, and two monothiols, decane-1-thiol ($C_{10}$) and octadecane-1-thiol ($C_{18}SH$), were used in this study. Conformations were generated using an energy minimization using molecular mechanics 2 (MM2) force field in Chem3D. Sulfur, carbon, hydrogen, and oxygen atoms are represented by yellow, gray, white, and red spheres, respectively.

techniques. First, high-resolution scanning tunneling microscopy (STM) was utilized to reveal surface morphology and structure of OPDT SAMs, under ultrahigh vacuum (UHV). Then, atomic force microscopy (AFM) imaging and nanografting were utilized to determine the thickness of the OPDT SAMs. Finally, well-ordered structures of low-coverage OPDT SAMs were produced by annealing the high-coverage SAMs in UHV, which served as our internal standards. The UHV-STM imaging revealed the location and arrangement of individual OPDT molecules on gold, as well as the order and periodicity of these internal standards, side by side. Comparisons of high-

resolution STM images of the internal standards and the OPDT SAMs yield the molecular-level structure of dithiol SAMs accurately and quantitatively. These results provide important insights into dithiol molecule−surface interactions, which benefits advanced applications of dithiol SAMs and are of fundamental importance for the research of dithiol SAMs and SAMs in general.[7−9,24−27]

## 2. METHODS

**2.1. Materials for Imaging and Structure Characterization.** Octadecane-1-thiol (abbreviated as $C_{18}SH$) (98%), and decane-1-thiol (abbreviated as $C_{10}SH$) (98%), were obtained from Sigma-Aldrich (St. Louis, MO) and used as received. The clear ruby muscovite mica substrate was purchased from Mica New York Corp (New York). Ethanol (200 proof), decalin (a mixture of cis and trans, 98%), hexane (≥99.9%), KOH, tetrahydrofuran (THF, purity ≥99.9%) were all purchased from Sigma-Aldrich. Deionized water (≥18.2 M$\omega$) was purified by a Milli-Q system (Q-GARD 2, Millipore Sigma, Billerica, MA). The STM tips were made from tungsten wires (purity 99.95%) purchased from California Fine Wire Company (Grover Beach, CA).

**2.2. Synthesis of (5-(Octyloxy)-1,3-phenylene)-dimethanethiol.** *Materials for Synthesis.* 3.5-Bis-(hydroxymethyl)phenol was prepared according to procedures available in the literature.[28] Potassium carbonate ($K_2CO_3$), methanesulfonyl chloride (MsCl), triethylamine ($Et_3N$), potassium thioacetate, lithium aluminum hydride ($LiAlH_4$), and 1-iodooctane were purchased from Sigma-Aldrich and used as received. The solvents tetrahydrofuran (THF) and dichloromethane ($CH_2Cl_2$) were purchased from Sigma-Aldrich. Hexanes, diethyl ether, acetonitrile ($CH_3CN$), and methanol (MeOH) were purchased from Mallinckrodt Chemicals. Anhydrous ethanol (EtOH) was purchased from Decon Laboratories, Inc. Distilling over calcium hydride gave

**Scheme 1. Synthesis of (5-(Octyloxy)-1,3-phenylene)dimethanethiol (OPDT)**
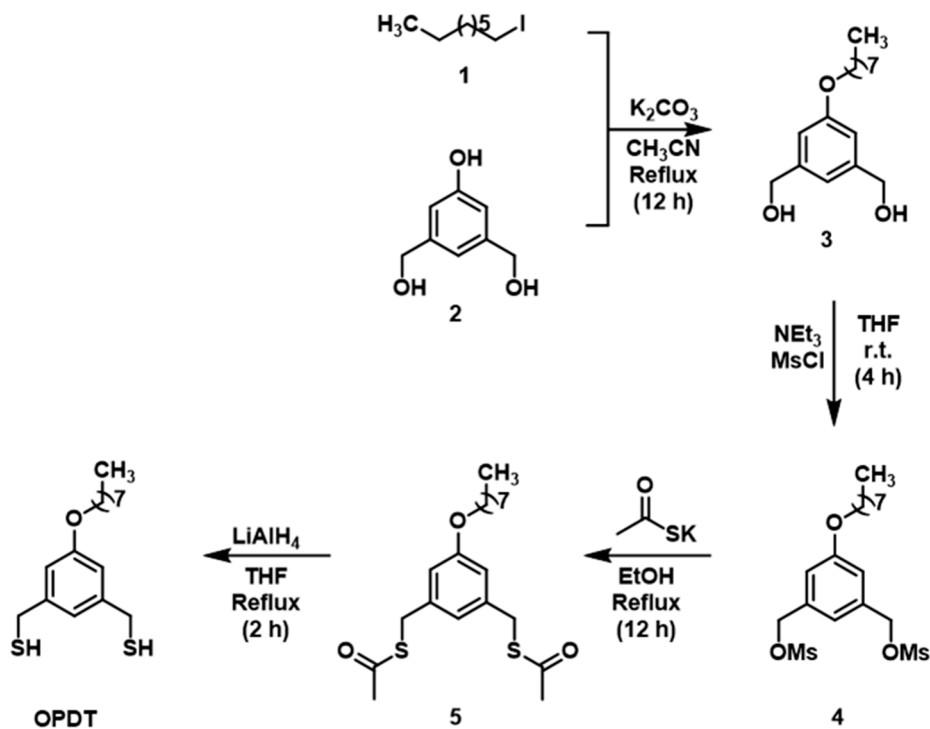
dry tetrahydrofuran and dichloromethane. Silica gel for column chromatography was obtained from Sorbent Technologies.

*Procedures.* (5-(Octyloxy)-1,3-phenylene)dimethanethiol (OPDT) was prepared using the steps outlined in Scheme 1. The experimental details are provided in the subsequent paragraphs.

*(5-(Octyloxy)-1,3-phenylene)dimethanol (3).* A mixture of $K_2CO_3$ (3.76 g, 20.0 mmol), 1-iodooctane (1.93 g, 8.04 mmol), and 3.5-bis(hydroxylmethyl)phenol (1.40 g, 9.09 mmol) in acetonitrile (250 mL) was refluxed for 12 h. The resulting mixture was condensed by rotary evaporation followed by the addition of diethyl ether (200 mL) and then acidification with 4.0 M HCl solution to afford a solution pH of ~3. The organic layer was washed with water (3 × 100 mL), dried over $Na_2SO_4$, and concentrated in vacuo to produce 1.90 g (7.14 mmol) of a white solid (89% yield). $^1$H NMR (500 MHz, CDCl$_3$): $\delta$ 6.24 (s, 1H), 6.84 (s, 2H), 4.66 (s, 4H), 3.96 (t, $J$ = 6.4 Hz, 2H), 1.76 (m, 2H), 1.25–1.43 (m, 26H), 0.87 (t, $J$ = 6.8 Hz, 3H).

*(5-(Octyloxy)-1,3-phenylene)bis(methylene) Dimethanesulfonate (4).* A 1.90 g (7.14 mmol) aliquot of (5-(octyloxy)-1,3-phenylene)dimethanol was introduced into a 500 mL round-bottomed flask containing 250 mL of THF, and then triethylamine (3.2 mL, 30 mmol) was added slowly to the mixture, which was stirred at room temperature for 30 min. The reaction flask was placed in an ice bath, and methanesulfonyl chloride (2.1 mL, 30 mmol) was transferred slowly to the solution while stirring. The ice bath was then removed, and the mixture was stirred for 4 h at room temperature. After completion of the reaction, excess methanesulfonyl chloride was destroyed by adding 100 mL of water followed by acidification with 4.0 M HCl solution to afford a solution pH of ~3. The mixture was extracted with diethyl ether (3 × 100 mL). The combined organic layers were washed with brine (100 mL) and water (3 × 100 mL). The organic layer was dried over $Na_2SO_4$, filtered, and concentrated in vacuo to produce (5-(octyloxy)-1,3-phenylene)bis-(methylene)dimethanesulfonate (2.70 g, 5.92 mmol), which was used in the next step without further purification (83% yield). $^1$H NMR (500 MHz, CDCl$_3$): $\delta$ 7.00 (s, 1H), 6.95 (s, 2H), 5.19 (s, 4H), 3.96 (t, $J$ = 6.4 Hz, 2H), 2.97 (s, 3H), 1.77 (m, 2H), 1.28–1.44 (m, 10H), 0.88 (t, $J$ = 7.3 Hz, 3H).

*S,S′-(5-(Octyloxy)-1,3-phenylene)bis(methylene) Diethanethioate (5).* A mixture of potassium thioacetate (1.71 g, 15.0 mmol) and (5-(octyloxy)-1,3-phenylene)bis(methylene) dimethanesulfonate (2.70 g, 5.92 mmol) in ethanol (300 mL) was refluxed for 12 h under nitrogen. After cooling, the precipitate was filtered off, rinsed with ethanol, and the combined organic phases were evaporated to dryness. The residue was taken up in a blend of diethyl ether (100 mL) and water (200 mL). The mixture was extracted with diethyl ether (2 × 100 mL). The combined organic layers were washed with brine (3 × 100 mL), dried over anhydrous $Na_2SO_4$, filtered, and concentrated by rotary evaporation, and then dried in vacuo to give 1.25 g (3.28 mmol) of S,S′-(5-(octyloxy)-1,3-phenylene)bis(methylene)diethanethioate as a yellow solid (55% yield). $^1$H NMR (500 MHz, CDCl$_3$): $\delta$ 6.75 (s, 1H), 6.69 (s, 2H), 4.03 (s, 4H), 3.89 (t, $J$ = 6.4 Hz, 2H), 2.33 (s, 6H), 1.77 (m, 2H), 1.25–1.44 (m, 10H), 0.87 (t, $J$ = 7.3 Hz, 3H).

*(5-(Octyloxy)-1,3-phenylene)dimethanethiol (OPDT).* To a suspension of LiAlH$_4$ (0.380 g, 10.0 mmol) in THF (300 mL) was added a solution of S,S′-(5-(octyloxy)-1,3-phenylene)bis-

(methylene) diethanethioate (1.25 g, 2.28 mmol) in THF (50 mL) dropwise at 0 °C. The ice bath was then removed, and the mixture was refluxed for 2 h under nitrogen. Subsequently, the reaction was quenched with degassed ethanol (25 mL). The mixture was acidified to pH ~ 1 by careful addition of 2.0 M HCl solution and then extracted with diethyl ether (3 × 100 mL). The combined organic layers were washed with brine (1 × 100 mL), dried over anhydrous $Na_2SO_4$, filtered, and concentrated by rotary evaporation. The crude product was purified by column chromatography (hexanes:ethyl acetate = 9.8:0.2) to give 0.605 g (2.18 mmol) of OPDT as a colorless oil (66% yield). $^1$H NMR (500 MHz, CDCl$_3$): $\delta$ 6.84 (s, 1H), 6.75 (s, 2H), 3.94 (t, $J$ = 6.3 Hz, 2H), 3.68 (d, $J$ = 8.0 Hz, 4H), 1.76 (m, 4H), 1.27–1.45 (m, 10H), 0.89 (t, $J$ = 6.3 Hz, 3H). $^{13}$C NMR (125 MHz, CDCl$_3$): $\delta$ 159.72, 143.00, 119.90, 112.96, 68.11, 31.94, 29.48, 29.38, 29.04, 26.18, 22.80, 14.27.

**2.3. Preparation of SAMs on Gold Thin Films.** Au(111) thin films were prepared in a high vacuum evaporator (DV-502A Thermal Evaporation system, Denton Vacuum, Moorestown, NJ).[23] The evaporation rate was 1.9 Å/s. The mica substrate was maintained at 673 K during Au deposition. After evaporation, the films were annealed at 673 K for 30 min. These protocols are known to yield Au(111) terraces, hundreds of nanometers in lateral dimensions.[23]

In parallel, a 1 mM decanethiol and a 1 mM octadecanethiol solution in ethanol were prepared. A 1 mM OPDT solution in THF was also prepared.[29] Mild sonication was used, if necessary, to accelerate the dissolution of the adsorbate. The Au thin films taken from the evaporator were cleaned using hydrogen flaming, then immediately immersed into the designated solutions (see above) for at least 24 h.[23] Prior to imaging, the surfaces of the thiol SAMs were washed with ethanol, hexane, then ethanol again. The samples were transferred to the designated sample stages for the STM and AFM investigations upon drying. The OPDT SAMs on Au(111) were washed sequentially with ethanol, decalin, hexane, and ethanol and then dried before being transferred to sample stages for STM or AFM investigations.

**2.4. STM Imaging and Structural Characterization.** Upon removal from the ethanolic OPDT solution and washing following the protocols described in Section 3 above, the OPDT SAMs were immediately mounted and transferred to the UHV STM chamber.[11,23] The STM tips used for this study were prepared by mechanically cutting tungsten wires, followed by electrochemical etching.[11,23] A home-constructed electrochemical potentiostat was used to control the redox reaction time and current to avoid over-etching.[11,23] The potentiostat monitored the redox current and automatically halted the etching process when the current dropped suddenly. Typical etching conditions were 2.1 V in a 3 M KOH solution.[23] The freshly fabricated tips were then washed sequentially with Milli-Q water and then ethanol several times. The tips were then quickly transferred to the UHV STM chamber.

A variable-temperature STM (STM 300, RHK Technology, Inc., Troy, MI) was employed for imaging. The STM was operated under UHV conditions with the background pressure in the UHV chamber maintained at 1 × 10$^{-10}$ mbar. A tungsten filament heater was mounted underneath the sample stage for annealing, and the final temperatures (300–398 K) were adjusted by varying the current. Temperatures were monitored using a thermocouple (K type) installed directly

underneath the sample to measure and monitor the annealing process.[11,23]

## 3. RESULTS AND DISCUSSION

**3.1. Production and Characterization of Striped Phases of OPDT SAMs.** Prior investigations by us and other researchers have found that alkanethiol SAMs at submonolayer coverage form striped phases on Au(111) surfaces.[11−15,30] In addition, aromatic thiols, such as 1,4-benzenedimethanethiol molecules, also formed striped phases on gold at low coverages.[20] These striped phases exhibit long-range order or periodicity.[10−13,15,16,22] Within these structures, thiols lie down on Au surfaces, and the chain−surface and chain−chain van der Waals interactions provide a basis for the formation of various striped structures.[10−15,20,23] Therefore, we hypothesized that the OPDT molecules would likely form striped structures at submonolayer coverages. By detaching a portion of the adsorbates with an OPDT SAM, we could create coexisting striped structures inlaid in the mature monolayer of OPDT SAM. The well-ordered striped phases would then provide good internal standards for the determination of the structures of the dithiol SAMs.

To prepare coexisting monolayer and submonolayer OPDT SAMs, we thermally heated OPDT SAMs under UHV to desorb a portion of the dithiols. To avoid under-or overheating, an iterative approach of "heating-cooling-imaging" was applied in our UHV-STM chamber, as illustrated in Figure 2A. For each heating event, STM images were acquired upon cooling to room temperature to assess desorption of OPDT in order to achieve coexisting monolayer and submonolayer coverage. Points i to v in Figure 2A indicate the times when the STM images were acquired. The chain length of our dithiol molecules is equivalent to tetradecanethiol, thus the melting

temperature and desorption should be ~80 and 130 °C, respectively, based on prior investigations of alkanethiols.[31,32] At 46 °C, which is significantly below the melting and desorption, annealing at 46 °C for 17 h aimed at the removal of loosely bond adsorbate molecules. At 76 °C, which is near but still below desorption, annealing at 76 °C for 43 h aimed at increasing the domain size of standing up domains and improving packing. At 120 °C, first annealing for 3 h aimed at partial desorption and formation of lying-down phase(s). second annealing for 16 h aimed at further desorption and increasing of the coverage of lying-down phase(s). The coverage of the standing-up and lying-down phases was calculated from the high-resolution STM images that taken after each sample annealing condition in Figure 2A, and results are shown in Figure 2B.

The synthesis (see Scheme S1) and characterization (see Sections S1 and S2) of OPDT are discussed in detail within the Supporting Information. OPDT SAMs were prepared by soaking gold thin films in 1 mM OPDT THF solution following established protocols.[2,4,5,18] Upon transferring inside the UHV chamber, STM imaging was performed at room temperature (point i in Figure 2) and base pressure of $1 \times 10^{-10}$ mbar. The typical surface morphology is shown in Figure 3A, where etch pits are visible and surrounded by packed but nearly randomly distributed OPDT molecules. The lack of long-range order is further revealed by the fast Fourier transform (FFT) shown in the inset of Figure 3A, where there are no ordered lattices. In contrast, a hexagonal lattice would result in the FFT image for alkanethiol SAMs on Au(111) surfaces which exhibit a well-known $c(4 \times 2)$ structure (see also Figure S3 in the Supporting Information).[13,14,16] Further heating led to a reduction in the number of etch pits, and sporadic stripes began to appear as shown in Figure 3B. Continued annealing led to more desorption of OPDT molecules or decreasing coverages and the formation of striped phases, as shown in Figure 3C, where an ordered domain with 11 stripes is visible in the central 40 nm × 15 nm area. The FFT image of the striped region is shown in the inset, where the two bright spots perpendicular to the stripes are visible, indicating long-range order or periodicity. Further annealing caused additional desorption and a further decrease in surface coverage; thus, more areas were covered by striped phases. These observations reveal that lowering the coverage of the solution prepared OPDT SAMs led to ordered structures (e.g., the striped phase) analogous to that observed in low-coverage monothiol SAMs.[11,13−16,20,22,30,33−35] The formation of the OPDT striped phases is highly reproducible, as we tested three batches of samples under various annealing conditions.
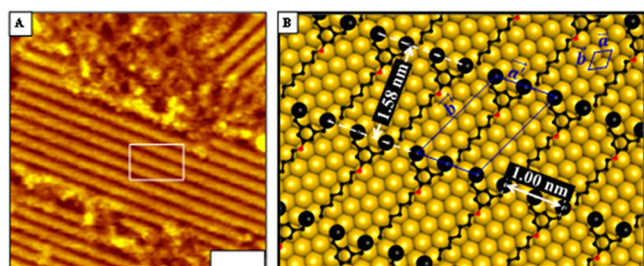
To determine the molecular-level structure of the OPDT striped phases, we collected high-resolution STM images as shown in Figure 4A. The stripes, corresponding to the S-headgroups, are aligned along the $\langle 121 \rangle$ direction, or the next nearest neighbor direction, of the Au(111) surface as illustrated in Figure 4B. The Au atoms in the Au(111) surface form a 2D closely packed structure (i.e., a hexagonal unit cell or unit mesh) with $a = b = 0.288$ nm as shown in Figure 4B.[12,36] The S atoms are likely located at the triple-hollow sites of the Au(111) lattice, from prior investigations on chemisorption of S on Au(111).[11,14,15] The interline distance in the STM image measures $1.52 \pm 0.08$ nm. Thus, we place the S-lines at 1.58 nm spacing to maintain that all S-headgroups reside at the triple hollow sites of Au(111). In
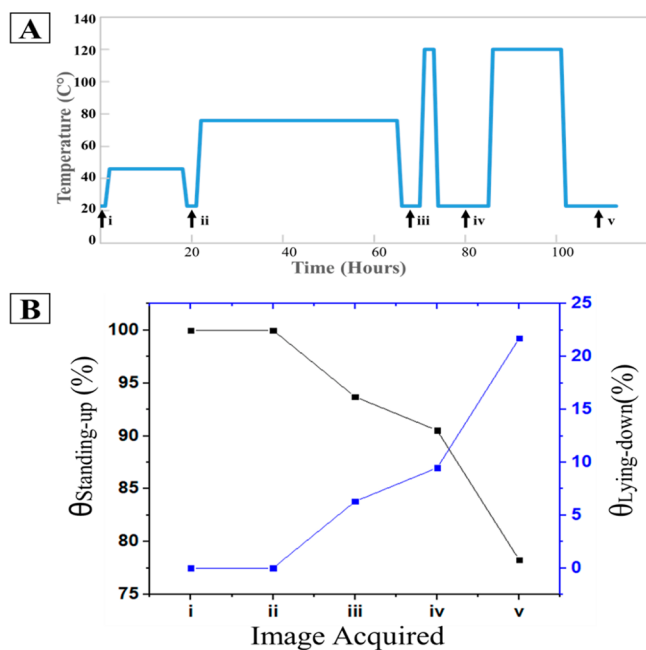
**Figure 2.** (A) Thermal desorption of OPDT from a SAM. Annealing process including designated temperatures and durations. Arrows i to v signify to the checking points where the OPDT SAMs were imaged by STM under UHV. (B) Coverage of standing-up phase ($\theta_{Standing}$, black) and lying-down phase ($\theta_{Lying-down}$, blue), measured from high-resolution STM topographic images.
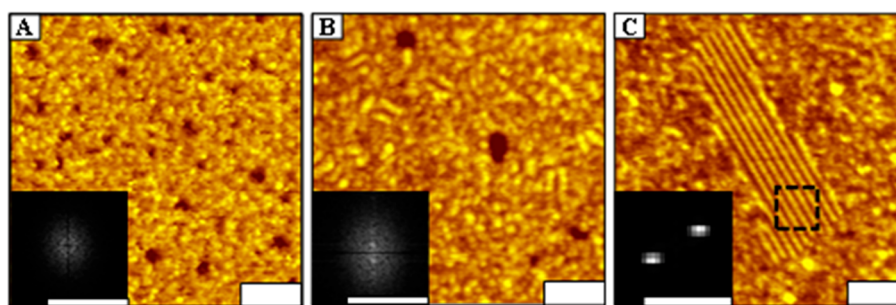
**Figure 3.** A 50 nm × 50 nm STM topographic image of an OPDT SAM after designed heating−cooling cycles. (A) OPDT SAM image under UHV without annealing (i.e., point i in Figure 2). Bias voltage $V$ = +1.4 V, and tunneling current $I$ = 10 pA. (B) STM image acquired at point iii in Figure 2 under $V$ = 1.4 V and $I$ = 20 pA. (C) STM image acquired at point iv in Figure 2 under $V$ = 1.4 V and $I$ = 10 pA. The scale bars in all STM images are 10 nm. Inserts are the corresponding 2D FFT of images over the entire scan in parts A and B, and over the striped region in part C. Scale bars on FFT images = 2 Gm$^{-1}$.
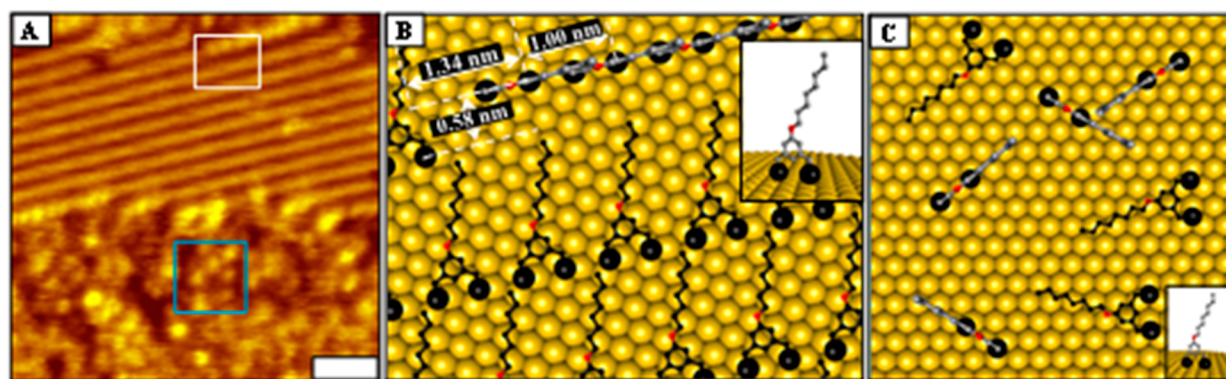


**Figure 4.** (A) A 30 nm × 30 nm STM topographic image of the OPDT SAM acquired at point v in Figure 2 under $V$ = −1.4 V and $I$ = 10 pA. (B) Molecular-level structure of the OPDT striped phase shown in reference to the Au(111) surface underneath (yellow spheres). The larger black spheres represent S headgroups, while the smaller black and red spheres represent C and O atoms, respectively. H atoms are omitted for clarity. The structure corresponds to the 6 nm × 4 nm area as indicated in part A.

other words, the striped phase is commensurate with the Au(111) lattice. Each OPDT molecule is likely lying flat on the surface with its aromatic ring and zigzag carbon plane parallel to the gold surface to maximize the van der Waals interactions between the molecule and the surface. Therefore, the striped phases are also referred to as "lying-down phases".[11,14,15,33−35,37] The unit cell or unit mesh of the

OPDT striped phase, $\vec{a}'$ and $\vec{b}'$, can be described with respect to that of Au(111) $\vec{a}$ and $\vec{b}$ using the universal notation as follows:

$$\begin{pmatrix} \vec{a}' \\ \vec{b}' \end{pmatrix} = \begin{pmatrix} 4 & 2 \\ -3 & 4 \end{pmatrix} \begin{pmatrix} \vec{a} \\ \vec{b} \end{pmatrix} \tag{1}$$

### 3.2. Molecular-Level Structural Characterization of OPDT SAMs.
With the striped structure well characterized and the coexistence of striped areas and high coverage OPDT SAM areas, we proceeded to use the striped structure as an internal standard or reference to facilitate the structural characterization of the high coverage OPDT SAMs. As the first step, we produced and characterized the 1D standing-up phase of the OPDT SAMs located next to the striped structures. In addition to the aforementioned striped structure, Figure 5A shows frequently occurring motifs, in each case, a line of well-resolved bright spots appearing at the end of a stripe. The image was acquired at point iv of Figure 2. These bright spots are either completely aligned with the corresponding stripe (middle left in Figure 5A) or with a small phase shift (upper right in Figure 5A). These 1D structures were always observed at the stripe boundaries and were sandwiched between the striped phase and the high-coverage phase. They also exhibited brighter contrast than the striped



**Figure 5.** (A) A 50 nm × 50 nm STM topographic image of the OPDT SAM acquired at point iv in Figure 2, under V = −1.4 V, and I = 10 pA. (B) Molecular level structure of the 1D standing up phase and the striped phase shown in reference to the Au(111) surface underneath. The striped structure follows the notation used in Figure 4B, and we use a gray color to represent C atoms in the standing-up phase to distinguish from C atoms in the lying-down phase (black). The structure corresponds to the 5 nm × 4 nm white frame as indicated in part A. (C) Molecular-level structure of the high coverage OPDT SAM within the 5 nm × 5 nm area as indicated in part A (teal frame). Insets are a side view indicating the orientation of the standing-up OPDT molecules with respect to the Au(111) surface.
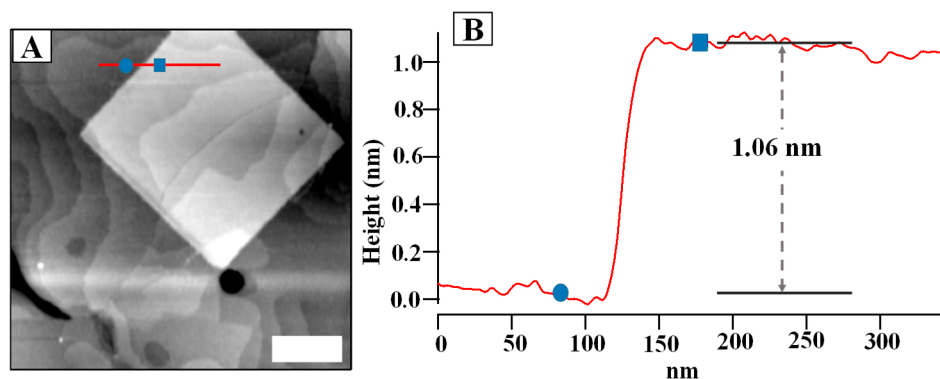
**Figure 6.** (A) A 1000 nm × 1000 nm AFM topographic image of an OPDT SAM within which a 500 × 600 nm area of $C_{18}SH$ SAM was produced using nanografting. Scale bar = 200 nm. (B) Cursor profile as indicated in part A revealing the height difference between the C18 and OPDT SAMs.

structures in the STM topographs. The distance between the spots measured 1.08 ± 0.09 nm, consistent with the intermolecular spacing of OPDT of 1.00 nm when closely packed together with the S headgroups aligned along the ⟨121⟩ direction of the Au(111) surface as shown in Figure 5B. Therefore, we infer that these 1D structures are ordered and standing-up OPDT molecules. Taking the area defined in Figure 5A as an example, the 1D standing-up structure shifted further from the stripe by 0.50 ± 0.06 nm along the ⟨101⟩ direction, and 1.39 ± 0.16 nm along the ⟨121⟩ direction of Au(111). Considering that the S headgroups occupy the triple hollow site of Au(111), the 1D standing-up OPDT structure is shown in Figure 5B in reference to the striped phase and Au(111) surface underneath. The standing-up configuration is illustrated in the inset of Figure 5B, where the aromatic ring is perpendicular to the Au(111) surface, and the zigzag plane of the chain is in the same plane defined by the aromatic ring.

The STM contrast of SAMs depends sensitively on the local density of states (LDOS) of the S atom chemisorbed on gold surfaces. The contrast is known to vary, depending on the actual structures (or phase);[12,23] e.g., in the case of alkanethiol SAMs, the S is well resolved for molecules in the standing-up phase with closely packed structure, but not always clearly resolved among lying-down phases, such as the M4 phase.[23] STM contrast also varies depending on the orientation of adsorbates, e.g., among standing-up decanethiol molecules.[12,23] It is fortunate, in the case of OPDT SAMs, that the standing-up molecules at the domain boundaries were clearly resolved, serving as an internal standard for structural determination of OPDT SAMs.

In the next step, we analyzed the STM images from low to high coverage, and identified those containing all three phases: striped, 1D standing up, and as prepared OPDT SAMs. Figure 5A provides an example where all three phases were captured in one image. Spot-like features are observed throughout the high coverage region (bottom half of Figure 5A), although these features appear randomly distributed with various contrasts. The contrast of the bright features in the high-coverage area is similar to that of the standing-up OPDT molecules, while the other features are attributed to the lying-down dithiol molecules. In the area defined by the 5 nm × 5 nm teal frame shown in Figure 5A, four bright and three dimmer features are present. Therefore, these bright and dimmer features are likely due to the standing-up and lying-down OPDT molecules, respectively. The distance between these OPDT molecules can be measured using the striped

phase and the 1D standing-up phase as internal standards. Considering that the S headgroups occupy the triple hollow site of Au(111), a structural model is constructed in Figure 5C to represent the OPDT SAMs prepared in solution.

Corroborating evidence was obtained from our AFM investigations, where we produced alkanethiol SAMs inlaid in OPDT SAMs using nanografting.[38,39] Figure 6 shows an AFM topographic image, where a 500 × 600 nm area of an octadecanethiol ($C_{18}SH$) SAM was inlaid in an OPDT SAM. Both SAMs exhibited homogeneous contrast because the AFM lateral resolution is lower than that of STM in general.[40,41] The single atomic steps of gold (lines in Figure 6A) are visible, demonstrating atomic level vertical resolution in this AFM image. The $C_{18}$ SAM region measures 1.06 ± 0.06 nm taller (Figure 6B) than the surrounding OPDT SAM. Since the $C_{18}$ SAM structure is well-known, including its height of 2.29 nm (see Figure S4),[11,39,42] the apparent height of the OPDT SAM is therefore 1.24 ± 0.06 nm (see Figure S5).[38,42] Assuming no tilt, the OPDT molecules should be 1.83 nm above Au(111) and, thus, taller than the height measured by AFM. The AFM apparent height measurements are consistent with our conclusion shown in Figure 5C, where the OPDT SAM is actually a mixture of standing-up (1.83 nm) and lying-down (0.5 nm) adsorbates. The height measured in AFM under contact mode imaging, therefore, falls in between the two configurations. Assuming a simple linear relationship, the estimated mixing would be 55.5% standing-up and 44.5% lying-down OPDT molecules, which is consistent with STM results shown in Figure 5.

## 4. CONCLUSIONS

With two −$CH_2$−SH groups at the meta positions of the aromatic ring, the chemisorption of OPDT intrinsically differs from that of n-alkanethiols on gold surfaces. Using high-resolution STM imaging under UHV in conjunction with creating and characterizing internal standards, this work revealed molecular-level packing of OPDT on Au(111) surfaces. The OPDT SAMs consist of a mixture of standing-up and lying-down molecules randomly distributed on Au(111), as illustrated in Figure 5C; thus, the SAMs have no long-rang order or ordered domains. The two thiols of each individual OPDT molecule occupy the triple hollow sites on Au(111). In the standing-up configuration, the benzene ring is perpendicular to the surface. In the lying-down configuration, the benzene ring and zigzag plane of the alkyl chain are parallel

to the Au(111) surface. Desorption of the OPDT SAMs leads to the formation of ordered domains known as the striped phases, whose unit mesh is quantified by eq 1. At the boundaries of these ordered structures, standing-up OPDT molecules are frequently present and aligned along the stripe directions with intermolecular spacing of 1 nm (i.e., 1D ordered and closely packed structures). To the best of our knowledge, this work is among the highest resolution, i.e., molecular-level characterization of dithiol SAMs, which is of fundamental importance to dithiol SAMs specifically and SAMs in general. The results also provide an important structural basis for dithiol molecule−surface interactions, which deepens our understanding of the unique properties of these SAMs.

## ■ ASSOCIATED CONTENT

### ⓈⒾ Supporting Information

The Supporting Information is available free of charge at https://pubs.acs.org/doi/10.1021/acs.jpcc.1c07171.

> Experimental details of OPDT synthesis, AFM in conjunction with nanografting, STM imaging following the "heating-cooling-imaging" protocols, and formation of striped phases (PDF)

## ■ AUTHOR INFORMATION

### Corresponding Authors

Gang-yu Liu − Department of Chemistry, University of California, Davis, California 95616, United States; Biophysics Graduate Group, University of California, Davis, California 95616, United States; ⓞ orcid.org/0000-0003-3689-0685; Phone: (530) 754-9678; Email: gyliu@ucdavis.edu; Fax: (530) 752-8995

T. Randall Lee − Department of Chemistry and the Texas Center for Superconductivity, University of Houston, Houston, Texas 77204, United States; ⓞ orcid.org/0000-0001-9584-8861; Email: trlee@uh.edu

### Authors

Umit Celik − Department of Chemistry, University of California, Davis, California 95616, United States

Han Ju Lee − Department of Chemistry and the Texas Center for Superconductivity, University of Houston, Houston, Texas 77204, United States

Terell Keel − Department of Chemistry, University of California, Davis, California 95616, United States

Logan A. Swartz − Biophysics Graduate Group, University of California, Davis, California 95616, United States

Marshall Van Zijll − Department of Chemistry, University of California, Davis, California 95616, United States

Cody J. Chalker − Department of Chemistry, University of California, Davis, California 95616, United States

Complete contact information is available at:
https://pubs.acs.org/10.1021/acs.jpcc.1c07171

### Notes

The authors declare no competing financial interest.

## ■ ACKNOWLEDGMENTS

## ■ REFERENCES

(1) Srisombat, L.; Jamison, A. C.; Lee, T. R. Stability: A key issue for self-assembled monolayers on gold as thin-film coatings and nanoparticle protectants. Colloids Surf., A 2011, 390 (1-3), 1−19.

(2) Rittikulsittichai, S.; Park, C. S.; Marquez, M. D.; Jamison, A. C.; Frank, T.; Wu, C.-H.; Wu, J. I.; Lee, T. R. Inhibiting Reductive Elimination as an Intramolecular Disulfide Dramatically Enhances the Thermal Stability of SAMs on Gold Derived from Bidentate Adsorbents. Langmuir 2018, 34 (23), 6645−6652.

(3) Lee, H. J.; Jamison, A. C.; Lee, T. R. Two Are Better than One: Bidentate Adsorbates Offer Precise Control of Interfacial Composition and Properties. Chem. Mater. 2016, 28 (15), 5356−5364.

(4) Garg, N.; Lee, T. R. Self-Assembled Monolayers Based on Chelating Aromatic Dithiols on Gold. Langmuir 1998, 14 (14), 3815−3819.

(5) Shon, Y.-S.; Lee, T. R. Desorption and Exchange of Self-Assembled Monolayers (SAMs) on Gold Generated from Chelating Alkanedithiols. J. Phys. Chem. B 2000, 104 (34), 8192−8200.

(6) Chinwangso, P.; Jamison, A. C.; Lee, T. R. Multidentate Adsorbates for Self-Assembled Monolayer Films. Acc. Chem. Res. 2011, 44 (7), 511−519.

(7) Park, C. S.; Lee, H. J.; Jamison, A. C.; Lee, T. R. Robust Thick Polymer Brushes Grafted from Gold Surfaces Using Bidentate Thiol-Based Atom-Transfer Radical Polymerization Initiators. ACS Appl. Mater. Interfaces 2016, 8 (8), 5586−5594.

(8) Lee, H. J.; Jamison, A. C.; Lee, T. R. Entropy-Driven Conformational Control of $\alpha,\omega$-Difunctional Bidentate-Dithiol Azo-Based Adsorbates Enables the Fabrication of Thermally Stable Surface-Grafted Polymer Films. ACS Appl. Mater. Interfaces 2016, 8 (24), 15691−15699.

(9) Hoang, J.; Park, C. S.; Lee, H. J.; Marquez, M. D.; Zenasni, O.; Gunaratne, P. H.; Lee, T. R. Quaternary Ammonium-Terminated Films Formed from Mixed Bidentate Adsorbates Provide a High-Capacity Platform for Oligonucleotide Delivery. ACS Appl. Mater. Interfaces 2018, 10 (47), 40890−40900.

(10) Riposan, A.; Liu, G.-y. Significance of local density of states in the scanning tunneling microscopy imaging of alkanethiol self-assembled monolayers. J. Phys. Chem. B 2006, 110 (47), 23926−23937.

(11) Yang, G.; Liu, G.-y. New Insights for Self-Assembled Monolayers of Organothiols on Au(111) Revealed by Scanning Tunneling Microscopy. J. Phys. Chem. B 2003, 107 (34), 8746−8759.

(12) Poirier, G. E. Mechanism of Formation of Au Vacancy Islands in Alkanethiol Monolayers on Au(111). Langmuir 1997, 13 (7), 2019−2026.

(13) Poirier, G. E. Coverage-Dependent Phases and Phase Stability of Decanethiol on Au(111). Langmuir 1999, 15 (4), 1167−1175.

(14) Poirier, G. E. Characterization of Organosulfur Molecular Monolayers on Au(111) using Scanning Tunneling Microscopy. Chem. Rev. 1997, 97 (4), 1117−1128.

(15) Poirier, G. E.; Pylant, E. D. The Self-Assembly Mechanism of Alkanethiols on Au(111). Science 1996, 272 (5265), 1145−1148.

(16) Poirier, G. E.; Tarlov, M. J. The c(4 × 2) Superlattice of n-Alkanethiol Monolayers Self-Assembled on Au(111). Langmuir 1994, 10 (9), 2853−2856.

(17) Love, J. C.; Estroff, L. A.; Kriebel, J. K.; Nuzzo, R. G.; Whitesides, G. M. Self-Assembled Monolayers of Thiolates on Metals as a Form of Nanotechnology. Chem. Rev. 2005, 105 (4), 1103−1170.

(18) Park, J.-S.; Smith, A. C.; Lee, T. R. Loosely Packed Self-Assembled Monolayers on Gold Generated from 2-Alkyl-2-methyl-propane-1,3-dithiols. Langmuir 2004, 20 (14), 5829−5836.

(19) Stranick, S. J.; Kamna, M. M.; Krom, K. R.; Parikh, A. N.; Allara, D. L.; Weiss, P. S. Scanning tunneling microscopy studies of self-assembled monolayers of alkanethiols on gold. *J. Vac. Sci. Technol., B: Microelectron. Process. Phenom.* **1994**, *12* (3), 2004−2007.

(20) Sharif, A. M.; Laffir, F. R.; Buckley, D. N.; Silien, C. Distinct self-assembly of dithiol monolayers on Au(111) in water and hexane. *Chem. Phys.* **2014**, *441*, 77−82.

(21) Yu, J.-J.; Ngunjiri, J. N.; Kelley, A. T.; Garno, J. C. Nanografting versus Solution Self-Assembly of α,ω-Alkanedithiols on Au(111) Investigated by AFM. *Langmuir* **2008**, *24* (20), 11661−11668.

(22) Leung, T. Y. B.; Gerstenberg, M. C.; Lavrich, D. J.; Scoles, G.; Schreiber, F.; Poirier, G. E. 1,6-Hexanedithiol Monolayers on Au(111): A Multitechnique Structural Study. *Langmuir* **2000**, *16* (2), 549−561.

(23) Qian, Y.; Yang, G.; Yu, J.; Jung, T. A.; Liu, G.-y. Structures of Annealed Decanethiol Self-Assembled Monolayers on Au(111): an Ultrahigh Vacuum Scanning Tunneling Microscopy Study. *Langmuir* **2003**, *19* (15), 6056−6065.

(24) Kim, S. Y.; Cho, S. J.; Byeon, S. E.; He, X.; Yoon, H. J. Self-Assembled Monolayers as Interface Engineering Nanomaterials in Perovskite Solar Cells. *Adv. Energy Mater.* **2020**, *10* (44), 2002606.

(25) Fahlman, M.; Fabiano, S.; Gueskine, V.; Simon, D.; Berggren, M.; Crispin, X. Interfaces in organic electronics. *Nature Reviews Materials* **2019**, *4* (10), 627−650.

(26) Casalini, S.; Bortolotti, C. A.; Leonardi, F.; Biscarini, F. Self-assembled monolayers in organic electronics. *Chem. Soc. Rev.* **2017**, *46* (1), 40−71.

(27) Casalini, S.; Leonardi, F.; Bortolotti, C. A.; Operamolla, A.; Omar, O. H.; Paltrinieri, L.; Albonetti, C.; Farinola, G. M.; Biscarini, F. Mono/bidentate thiol oligoarylene-based self-assembled monolayers (SAMs) for interface engineering. *J. Mater. Chem.* **2012**, *22* (24), 12155−12163.

(28) Lee, H. J.; Jamison, A. C.; Yuan, Y.; Li, C.-H.; Rittikulsittichai, S.; Rusakova, I.; Lee, T. R. Robust Carboxylic Acid-Terminated Organic Thin Films and Nanoparticle Protectants Generated from Bidentate Alkanethiols. *Langmuir* **2013**, *29* (33), 10432−10439.

(29) Hutter, J. L. Comment on Tilt of Atomic Force Microscope Cantilevers: Effect on Spring Constant and Adhesion Measurements. *Langmuir* **2005**, *21* (6), 2630−2632.

(30) Guo, Q.; Li, F. Self-assembled alkanethiol monolayers on gold surfaces: resolving the complex structure at the interface by STM. *Phys. Chem. Chem. Phys.* **2014**, *16* (36), 19074−19090.

(31) Ishida, T.; Fukushima, H.; Mizutani, W.; Miyashita, S.; Ogiso, H.; Ozaki, K.; Tokumoto, H. Annealing Effect of Self-Assembled Monolayers Generated from Terphenyl Derivatized Thiols on Au(111). *Langmuir* **2002**, *18* (1), 83−92.

(32) Ramin, L.; Jabbarzadeh, A. Odd−Even Effects on the Structure, Stability, and Phase Transition of Alkanethiol Self-Assembled Monolayers. *Langmuir* **2011**, *27* (16), 9748−9759.

(33) Hamoudi, H.; Prato, M.; Dablemont, C.; Cavalleri, O.; Canepa, M.; Esaulov, V. A. Self-Assembly of 1,4-Benzenedimethanethiol Self-Assembled Monolayers on Gold. *Langmuir* **2010**, *26* (10), 7242−7247.

(34) Stammer, X.; Tonigold, K.; Bashir, A.; Käfer, D.; Shekhah, O.; Hülsbusch, C.; Kind, M.; Groß, A.; Wöll, C. A highly ordered, aromatic bidentate self-assembled monolayer on Au(111): a combined experimental and theoretical study. *Phys. Chem. Chem. Phys.* **2010**, *12* (24), 6445−6454.

(35) Vericat, C.; Vela, M. E.; Benitez, G.; Carro, P.; Salvarezza, R. C. Self-assembled monolayers of thiols and dithiols on gold: new challenges for a well-known system. *Chem. Soc. Rev.* **2010**, *39* (5), 1805−1834.

(36) Wöll, C.; Chiang, S.; Wilson, R. J.; Lippel, P. H. Determination of atom positions at stacking-fault dislocations on Au(111) by scanning tunneling microscopy. *Phys. Rev. B: Condens. Matter Mater. Phys.* **1989**, *39* (11), 7988−7991.

(37) Jia, J.; Mukherjee, S.; Hamoudi, H.; Nannarone, S.; Pasquali, L.; Esaulov, V. A. Lying-Down to Standing-Up Transitions in Self Assembly of Butanedithiol Monolayers on Gold and Substitutional Assembly by Octanethiols. *J. Phys. Chem. C* **2013**, *117* (9), 4625−4631.

(38) Liu, G.-Y.; Xu, S.; Qian, Y. Nanofabrication of Self-Assembled Monolayers Using Scanning Probe Lithography. *Acc. Chem. Res.* **2000**, *33* (7), 457−466.

(39) Xu, S.; Liu, G.-y. Nanometer-Scale Fabrication by Simultaneous Nanoshaving and Molecular Self-Assembly. *Langmuir* **1997**, *13* (2), 127−129.

(40) Lüthi, R.; Meyer; Bammerlin, M.; Baratoff, A.; Lü, J.; Guggisberg, M.; Güntherodt, H. J. Resolution Limits of Force Microscopy. *ACS Symp. Ser.* **1998**, 300−311.

(41) Bottomley, L. A.; Coury, J. E.; First, P. N. Scanning Probe Microscopy. *Anal. Chem.* **1996**, *68* (12), 185−230.

(42) Fenter, P.; Eberhardt, A.; Eisenberger, P. Self-Assembly of Alkyl Thiols as Disulfides on Au(111). *Science* **1994**, *266* (5188), 1216.